

Electrically driven nanopyramid green light emitting diode

S.-P. Chang, Y.-C. Chen, J.-K. Huang, Y.-J. Cheng, J.-R. Chang, K.-P. Sou, Y.-T. Kang, H.-C. Yang, T.-C. Hsu, H.-C. Kuo, and C.-Y. Chang

Citation: [Applied Physics Letters](#) **100**, 061106 (2012); doi: 10.1063/1.3681363

View online: <http://dx.doi.org/10.1063/1.3681363>

View Table of Contents: <http://scitation.aip.org/content/aip/journal/apl/100/6?ver=pdfcov>

Published by the [AIP Publishing](#)

Articles you may be interested in

[Green cubic GaInN/GaN light-emitting diode on microstructured silicon \(100\)](#)

Appl. Phys. Lett. **103**, 232107 (2013); 10.1063/1.4841555

[Defect-reduced green GaInN/GaN light-emitting diode on nanopatterned sapphire](#)

Appl. Phys. Lett. **98**, 151102 (2011); 10.1063/1.3579255

[Enhanced efficiency and reduced spectral shift of green light-emitting-diode epitaxial structure with prestrained growth](#)

J. Appl. Phys. **104**, 123106 (2008); 10.1063/1.3046582

[Carrier recombination mechanisms in nitride single quantum well light-emitting diodes revealed by photo- and electroluminescence](#)

J. Appl. Phys. **104**, 094504 (2008); 10.1063/1.3009335

[Bright semipolar Ga In N Ga N blue light emitting diode on side facets of selectively grown GaN stripes](#)

Appl. Phys. Lett. **89**, 041121 (2006); 10.1063/1.2240307

The advertisement features a dark blue background with white and orange text. At the top left, it reads 'NEW! Asylum Research MFP-3D Infinity™ AFM' in large white letters, followed by 'Unmatched Performance, Versatility and Support' in orange. The Oxford Instruments logo is in the top right corner, with the tagline 'The Business of Science®' below it. The central part of the ad is divided into four quadrants, each with an image and text: top-left shows a blue textured surface with 'Stunning high performance'; top-right shows a brown textured surface with 'Simpler than ever to GetStarted™'; bottom-left shows a patterned surface with 'Comprehensive tools for nanomechanics'; bottom-right shows a tray of colorful samples with 'Widest range of accessories for materials science and bioscience'. On the far right, there is an image of the MFP-3D Infinity AFM instrument.

Electrically driven nanopyramid green light emitting diode

S.-P. Chang,^{1,2} Y.-C. Chen,¹ J.-K. Huang,¹ Y.-J. Cheng,^{1,3,a)} J.-R. Chang,⁴ K.-P. Sou,¹ Y.-T. Kang,¹ H.-C. Yang,² T.-C. Hsu,² H.-C. Kuo,¹ and C.-Y. Chang⁴

¹Department of Photonics and Institute of Electro-Optical Engineering, National Chiao Tung University, 1001 Ta Hsueh Rd., Hsinchu 300, Taiwan

²R&D Division, Epistar Co. Ltd., Science-based Industrial Park, Hsinchu 300, Taiwan

³Research Center for Applied Sciences, Academia Sinica, Taipei 11529, Taiwan

⁴Department of Electronic Engineering, National Chiao Tung University, 1001 Ta Hsueh Rd., Hsinchu 300, Taiwan

(Received 27 August 2011; accepted 13 January 2012; published online 7 February 2012)

An electrically driven nanopyramid green light emitting diode (LED) was demonstrated. The nanopyramid arrays were fabricated from a GaN substrate by patterned nanopillar etch, pillar side wall passivation, and epitaxial regrowth. Multiple quantum wells were selectively grown on the facets of the nanopyramids. The fabricated LED emits green wavelength under electrical injection. The emission exhibits a less carrier density dependent wavelength shift and higher internal quantum efficiency as compared with a reference c-plane sample at the same wavelength. It shows a promising potential for using nanopyramid in high In content LED applications. © 2012 American Institute of Physics. [doi:10.1063/1.3681363]

Light emitting semiconductor devices in green color have attracted great interests in lighting and projection display applications.^{1–3} GaN based light emitting diodes (LEDs) are often fabricated on c-plane GaN surface. The emission is typically in the blue region, where its performance is optimal. Multiple quantum wells (MQWs) grown on this crystal plane experience an internal electric field (IEF) due to spontaneous and piezoelectric polarization, which can significantly reduce internal quantum efficiency (IQE).^{4,5} The efficiency drops rapidly as In content increases in MQWs for green emission due to the increased IEF.⁶ This IEF can also cause carrier density dependent wavelength shift. To overcome these detrimental effects, an attractive approach is to grow MQWs on nonpolar or semipolar crystal planes, which have no or lower IEF and can accommodate high In incorporation.⁷ Green LEDs and lasers fabricated on semipolar GaN substrates have gained significant interests recently.^{8–12} However, nonpolar and semipolar substrates are not readily available.

Selective area growth is an attractive alternative method to grow semipolar facets from the widely available c-plane substrates. Micro to nano size hexagonal pyramids can be grown from the opening holes of a SiO_x or SiN_x masked c-plane GaN substrate. The pyramid facets are typically {10-11} or {11-22} semipolar planes. The photoluminescent (PL) study of the MQWs grown on semipolar pyramid facets has shown significantly reduced the carrier density dependent wavelength shift and inhomogeneous In distribution.^{13,14} There have been interests in using the semipolar pyramid facets for green InGaN LED applications,^{13–16} but so far the reports are mostly limited to optical pumping. Reports on electrical injection are very limited.¹⁶ Here, we report the fabrication and performance of an electrically driven nanopyramid green LED. Compared with a reference c-plane

MQW LED, the PL measurement has shown less carrier density dependent blue shift and significantly enhanced IQE.

The device was fabricated from an n-type GaN substrate grown on a c-plane sapphire template by AXITRON 2000HT metal organic chemical vapor deposition (MOCVD) reactor. The scanning electron microscopy (SEM) images of the intermediate fabrication steps are shown in Figs. 1(a)–1(d). SiO₂ nano disks of 250 μm in diameter were first patterned on a GaN substrate. The SiO₂ disks were used as etching masks in inductively coupled plasma reactive ion etching (RIE). The SiO₂ disks were subsequently removed by a buffer oxide etch, leaving arrays of GaN nanopillars (Fig. 1(a)). Spin-on glass was spun on the substrate to planarize the surface. After curing the spin-on glass at 400 °C for 60 min, the nanopillar side walls were covered by spin-on glass with air voids among them. The air voids were created due to the shrinkage of spin-on glass during curing process. The substrate was then etched by RIE to expose the top portion of nanopillars while leaving nanopillar side walls still covered with spin-on glass (Fig. 1(b)). The substrate was put back into MOCVD for GaN epitaxial regrowth. GaN pyramids were selectively grown on the tops of nanopillars at growth pressure of 600 mbar and temperature of 800 °C with growth rate of about 0.5 μm/hr (Fig. 1(c)). The pyramid facets were identified as semipolar {10-11} plane from its inclined 62° angle. Ten pairs of In_{0.3}Ga_{0.7}N (~2 nm)/GaN (~8 nm) MQWs were grown on the pyramid facets, followed by a 20-nm electron blocking layer of Mg-doped p-type Al_{0.15}Ga_{0.85}N and a 200-nm Mg-doped p-type GaN layer. The growth temperature of GaN and InGaN was 800 °C and 710 °C, respectively. The MQW growth pressure was 300 mbar. The trimethylindium (TMIn) and trimethylgallium (TMGa) flux were 250 and 76 sccm, respectively. Figure 1(d) shows the plane view of the fabricated LED. The surface was rough due to the nanopyramid structure. For comparison, a conventional c-plane MQW substrate was grown on a c-plane sapphire template. The MQW growth parameters were similar

^{a)}Author to whom correspondence should be addressed. Electronic mail: yjcheng@sinica.edu.tw.

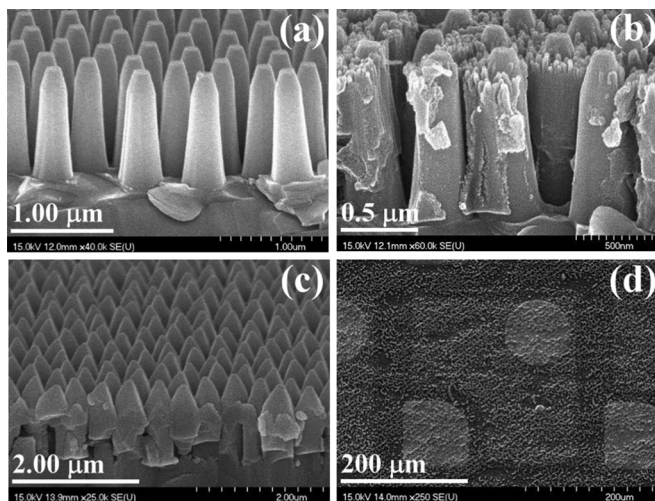


FIG. 1. (a)-(d) SEM images of intermediate fabrication steps. (a) Etched nanopillar. (b) Side wall coated with spin-on glass. (c) Nanopyramids grown on nanopillars (d) Plane view of nanopillar LED.

except that the barrier and well growth temperature were raised to 820 °C and 730 °C, respectively.

The emission properties of the fabricated {10-11} and {0001} MQW samples were investigated by PL measurement. The samples were optically excited by a Ti:sapphire pulse laser at wavelength of 400 nm focused down to a spot diameter of approximately 50 μm on the sample. The repetition rate was 76 MHz, and the pulse width was 0.2 ns. The measured PL peak wavelength versus excitation power density is shown in Fig. 2(a). The {0001} MQW sample had a blueshift of 45 nm when the pump intensity was increased from 1 W/cm² to 2.5 kW/cm². In contrast, the {10-11} MQW sample had a blueshift of only 10 nm within the same pump intensity range. The blueshift was due to the screening of IEF by the excited carriers and the filling of localized potential fluctuations induced by inhomogeneous In distribution in MQWs. The observed smaller blueshift of {10-11} MQWs is consistent with previous reports.^{13,14} The carrier life time was measured by a time resolved PL (TRPL) system (PicoHarp 300) at low temperature (LT) 15 K and room temperature (RT). The measured TRPL signals are shown in Figs. 3(a) and 3(b). The {10-11} sample exhibits a much shorter decay time constant than the {0001} sample does. The stretched exponential fits, $exp(-(t/\tau)^\beta)$, to the {10-11} sample at LT and RT are shown in Fig. 3(a). It gives a decay time constant τ of 0.16 and 0.11 ns and a dispersive component

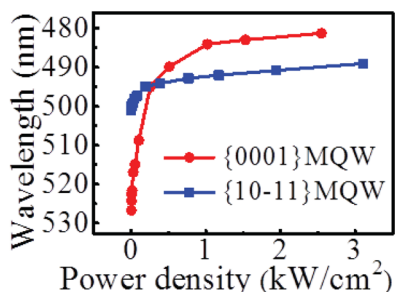


FIG. 2. (Color online) PL peak wavelength versus pump power density of {10-11} and {0001} MQWs.

of β of 0.71 and 0.97, respectively. The stretched exponential decay is often encountered in a disordered system. The dispersion component is a consequence of a distribution of decay time constants. This could be caused by the localized potentials formed by the inhomogeneous In distribution in MQWs. The increase of β value toward unity at RT indicates that the localized potentials are shallow potentials. The carriers can be excited from the localized states to extended states by thermal energy, leading to a narrower decay time constant distribution. Due to the limit of the repetition rate of pulse laser, the recorded transient PL intensity of the {0001} sample does not fully decay within one excitation period. This prohibits a direct curve fitting to obtain decay time constant. However, from the slow decay waveform as shown in Fig. 3(b), the decay time constant at LT and RT can be estimated around tens of ns and a few ns, respectively. The sub-nanosecond life time of {10-11} MQWs and tens of ns life time of {0001} MQWs at LT are consistent with previous reported values.¹⁷ Non-radiative recombination is normally inactive at low enough temperature. The measured LT life time is, therefore, assumed to be due to radiative recombination. The shorter life time of {10-11} MQWs is again attributed to the lower IEF, which results in better electron-hole wave function overlap and higher radiative recombination probability. At RT, the non-radiative recombination is normally not negligible, which causes the PL life time to become shorter and degrades the IQE.

We measured the IQEs of these two samples. The IQE was obtained by normalizing the integrated PL intensity at room temperature by the value at 15 K. The pump power was set at the level where the integrated PL intensity is at maximum at 15 K. The measured IQE of {10-11} and {0001} MQWs was 50% and 28%, respectively. It is worth to note that the IQE of {10-11} sample is enhanced only by 79%, which is in large disparity to the nearly two order of magnitude decrease in radiative lifetime, as compared with the {0001} sample. This discrepancy implies that the non-radiative recombination rate is also much faster for {10-11} sample. The much shorter τ_{nr} of {10-11} sample could be attributed to the less localized potential fluctuations, as compared with {0001} sample. Previous experimental results suggest that the localized potential due to inhomogeneous In distribution may suppress the capture of carriers by non-radiative centers.¹⁷⁻¹⁹ The reduced localized potential fluctuations of {10-11} MQW, therefore, increase the carrier capture probability by non-radiative centers and give shorter τ_{nr} .

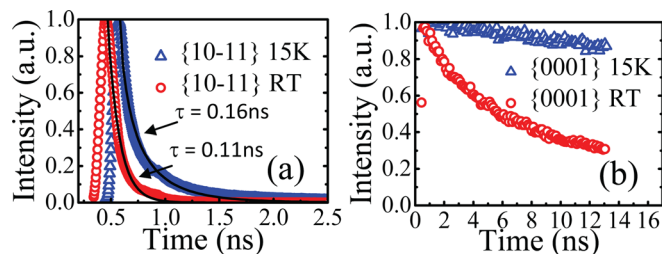


FIG. 3. (Color online) TRPL decay curves of (a) {10-11} and (b) {0001} MQWs at 15 K and RT. The solid lines are the fitted stretched exponential decay curves.

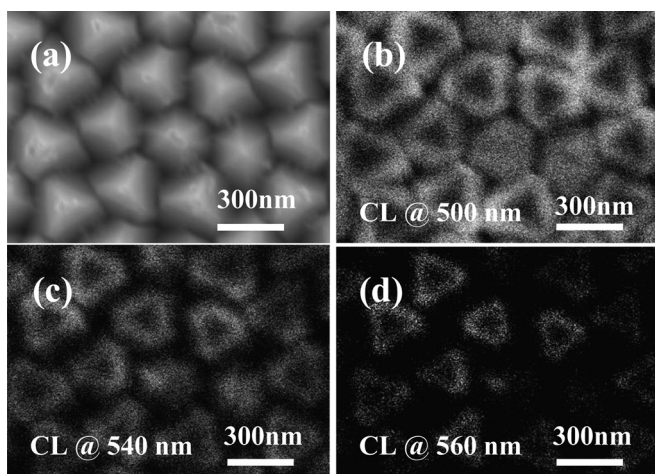


FIG. 4. (a) SEM plane view of nanopillar LED. (b)–(d) Spectrally resolved CL images at 500, 540, and 560 nm.

The spatial dependent emission property of nanopillars was investigated by the spectrally resolved cathodoluminescent (CL) measurement. A plane view scanning electron microscope (SEM) image was first taken, as shown in Fig. 4(a). The spectrally resolved CL images were then scanned at 500, 540, and 560 nm, as shown in Fig. 4(b)–4(d). The emission pattern basically follows the pyramid height contour, as can be seen by comparing the bright contours in Fig. 4(b)–4(d) to the pyramid shape in SEM image Fig. 4(a). The contours move toward the tip region of nanopillars as wavelength increases. It indicates that the MQW emission redshifts from the bottom to top region of nanopillars. This may be due to the increase of In incorporation and IEF in MQWs as the region moves up the nanopillar facets.

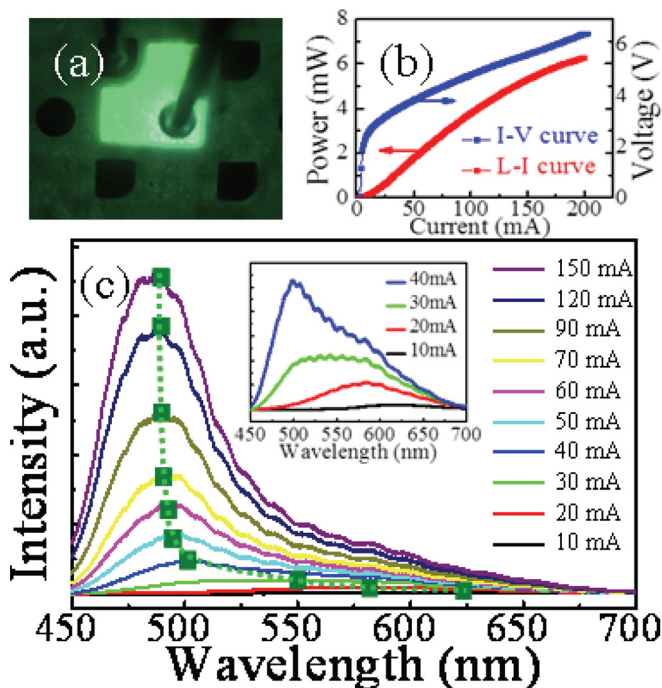


FIG. 5. (Color online) (a) Microscope image of electrically driven nanopillar green LED. (b) L-I-V curves of nanopillar LED. (c) PL spectrum versus injection current. Inset is the low current PL spectra.

The {10-11} MQW substrate was fabricated into a $300\ \mu\text{m} \times 300\ \mu\text{m}$ LED chip using standard LED fabrication steps. The microscope image of the electrically driven LED exhibits a bluish green emission as shown in Fig. 5(a). The dark regions are the p- and n-metal contacts. The light-current-voltage (L-I-V) curves of the fabricated nanopillar LED chip are shown in Fig. 5(b). The L-I curve shows a slow turn on of light. When the current is at 5 mA, the steep increase of voltage starts to level off at 2.3 V, while light output is still negligible. This is probably due to some growth defects and process imperfection that provide shunt paths to the current. The coalescent boundaries among nanopillars could be one of the possible causes. After turn on, the driving voltage increases substantially from 3 V to 7 V as current increases up to 200 mA. This high voltage is probably due to a high contact resistance between ITO and the non-planar surface of nanopillar arrays. Process optimization is required for a further improvement. The electroluminescent (EL) spectrum versus injection current is shown in Fig. 5(c). At low injection current, emission peak starts at 625 nm and blueshifts as current increases (inset of Fig. 5(c)). The emission peak is stabilized around 495 nm above 50 mA, as depicted by the dotted line. The spectrum has a broad linewidth of ~ 57 nm and a long tail extended beyond 600 nm. There are small Fabry-Perot oscillation ripples with ~ 8.25 nm spacing. It corresponds to a cavity length of $\sim 6\ \mu\text{m}$, which is close to the total GaN thickness. The ripple is probably due to the reflection between pyramid facets, acting like the effect of a corner cube, and the sapphire/GaN interface. From the CL measurement, the initial long wavelength emission is likely from the apex region of MQWs, which is turned on first because the potential is lower. As the current increases, the injected carriers overflow to the lower portion of MQWs. The emission thus shifts to 495 nm and becomes the dominant peak because of the much larger MQW area.

In summary, we have demonstrated an electrically driven nanopillar LED. The LED was fabricated from a patterned nanopillar etch, pillar side wall passivation, and MOCVD regrowth. MQWs were grown on the semipolar facets of the nanopillars. The semipolar MQWs were shown to have less carrier density dependent wavelength shift and higher IQE as compared with a c-plane sample with similar emission wavelength. This demonstration shows a promising potential for developing high In composition LEDs by using semipolar MQWs grown on nanopillars, which can be fabricated from readily available c-plane sapphire substrates.

The authors would like to thank Dr. T. C. Hsu and M. H. Shieh of Epistar Corporation for their technical supporting. This work was financially supported by the National Science Council of Taiwan under Contract No. NSC NSC97-2112-M-001-027-MY3.

¹K. S. Kim, J. K. Son, S. N. Lee, Y. J. Sung, H. S. Paek, H. K. Kim, M. Y. Kim, K. H. Ha, H. Y. Ryu, O. H. Nam *et al.*, *Appl. Phys. Lett.* **92**, 101103 (2008).

²D. Queren, A. Avramescu, G. Brüderl, A. Breidenassel, M. Schillgalies, S. Lutgen, and U. Strauß, *Appl. Phys. Lett.* **94**, 081119 (2009).

³T. Miyoshi, S. Masui, T. Okada, T. Yanamoto, T. Kozaki, S.-I. Nagahama, and T. Mukai, *Appl. Phys. Express* **2**, 062201 (2009).

⁴Y.-L. Lai, C.-P. Liu, Y.-H. Lin, R.-M. Lin, D.-Y. Lyu, Z.-X. Peng, and T.-Y. Lin, *Appl. Phys. Lett.* **89**, 151906 (2006).

- ⁵F. Bernardini, V. Fiorentini, and D. Vanderbilt, *Phys. Rev. B* **56**, R10024 (1997).
- ⁶D. Fuhrmann, C. Netzel, U. Rossow, A. Hangleiter, G. Ade, and P. Hinze, *Appl. Phys. Lett.* **88**, 071105 (2006).
- ⁷H. Sato, R. B. Chung, H. Hirasawa, N. Fellows, H. Masui, F. Wu, M. Saito, K. Fujito, J. S. Speck, S. P. DenBaars *et al.*, *Appl. Phys. Lett.* **92**, 221110 (2008).
- ⁸H. Zhong, A. Tyagi, N. N. Fellows, F. Wu, R. B. Chung, M. Saito, K. Fujito, J. S. Speck, S. P. DenBaars, and S. Nakamura, *Appl. Phys. Lett.* **90**, 233504 (2007).
- ⁹K. Okamoto, J. Kashiwagi, T. Tanaka, and M. Kubota, *Appl. Phys. Lett.* **94**, 071105 (2009).
- ¹⁰A. Tyagi, Y.-D. Lin, D. A. Cohen, M. Saito, K. Fujito, J. S. Speck, S. P. DenBaars, and S. Nakamura, *Appl. Phys. Express* **1**, 091103 (2008).
- ¹¹H. Asamizu, M. Saito, K. Fujito, J. S. Speck, S. P. DenBaars, and S. Nakamura, *Appl. Phys. Express* **1**, 091102 (2008).
- ¹²Y. Enya, Y. Yoshizumi, T. Kyono, K. Akita, M. Ueno, M. Adachi, T. Sumitomo, S. Tokuyama, T. Ikegami, K. Katayama *et al.*, *Appl. Phys. Express* **2**, 082101 (2009).
- ¹³T. Kim, J. Kim, M.-S. Yang, S. Lee, Y. Park, U.-I. Chung, and Y. Cho, *Appl. Phys. Lett.* **97**, 241111 (2010).
- ¹⁴H. Yu, L. K. Lee, T. Jung, and P. C. Ku, *Appl. Phys. Lett.* **90**, 141906 (2007).
- ¹⁵C. Liu, A. Satka, L. K. Jagadamma, P. R. Edwards, D. Allsopp, R. W. Martin, P. Shields, J. Kovac, F. Uherek, and W. Wang, *Appl. Phys. Express* **2**, 121002 (2009).
- ¹⁶I. H. Wildeson, R. Colby, D. A. Ewoldt, Z. Liang, D. N. Zakharov, N. J. Zaluzec, R. E. García, E. A. Stach, and T. D. Sands, *J. Appl. Phys.* **108**, 044303 (2010).
- ¹⁷M. Funatoa and Y. Kawakami, *J. Appl. Phys.* **103**, 093501 (2008).
- ¹⁸S. Chichibu, T. Azuhata, T. Sota, and S. Nakamura, *Appl. Phys. Lett.* **69**, 4188 (1996).
- ¹⁹S. Nakamura, *Science* **281**, 956 (1998).